Bioactive Materials 6 (2021) 1555–1562

Contents lists available at ScienceDirect

Bioactive Materials

journal homepage: www.sciencedirect.com/journal/bioactive-materials

Pollens derived magnetic porous particles for adsorption of low-density lipoprotein from plasma

Yuetong Wang [a,b,e], Lingyu Sun [a,b,e], Jiahui Guo [a,b,e], Keqing Shi [a], Luoran Shang [a,c,*], Jian Xiao [a,d,**], Yuanjin Zhao [a,b,e,***]

[a] Precision Medicine Center Laboratory, The First Affiliated Hospital of Wenzhou Medical University, Wenzhou, 325035, China
[b] Department of Clinical Laboratory, Institute of Translational Medicine, The Affiliated Drum Tower Hospital of Nanjing University Medical School, Nanjing, 210008, China
[c] Zhongshan-Xuhui Hospital, The Shanghai Key Laboratory of Medical Epigenetics, The International Co-laboratory of Medical Epigenetics and Metabolism, Ministry of Science and Technology, Institutes of Biomedical Sciences, Fudan University, Shanghai, 200032, China
[d] Research Units of Clinical Translation of Cell Growth Factors and Diseases Research of Chinese Academy of Medical Science, School of Pharmaceutical Science, Wenzhou Medical University, Wenzhou, China
[e] State Key Laboratory of Bioelectronics, School of Biological Science and Medical Engineering, Southeast University, Nanjing, 210096, China

ARTICLE INFO

Keywords:
Pollen
Microporous structure
Low-density lipoprotein
Oil/water separation
Lipid adsorption

ABSTRACT

Adsorption of low-density lipoprotein from plasma is vital for the treatment of dyslipidemia. Appropriate adsorbent material for efficient and selective adsorption of low-density lipoprotein is highly desired. In this work, we developed pollens-derived magnetic porous particles as adsorbents for this purpose. The natural pollen grains were modified to obtain high surface porosity, a large inner cavity, magnet responsiveness, and specific wettability. The resultant particles exhibited satisfying performance in the adsorption of a series of oils and organic solvents out of water. Besides, the particles were directly utilized to the adsorption of low-density lipoprotein in plasma, which showed high selectivity, and achieved an outstanding adsorption capacity as high as 34.9% within 2 h. Moreover, their salient biocompatibility was demonstrated through simulative hemoperfusion experiments. These features, together with its abundant source and facile fabrication, makes the pollens-derived magnetic porous particles excellent candidate for low-density lipoprotein -apheresis and water treatment applications.

1. Introduction

Cardiovascular disease (CVD) is one of the leading causes of mortality and is greatly related to dyslipidemia, for instance, hypercholesterolemia. It has been well established that the elevated level of low-density lipoprotein (LDL) undertakes the major risk factor and is thus indicative of atherosclerosis [1–4]. Diet and drug therapy could regulate the cholesterol level of most hypercholesterolemia patients. However, as for those who are resistant to drug therapy or suffering from familial hypercholesterolemia, LDL-apheresis has become the most efficient method by decreasing the LDL level in plasma [5,6]. LDL-apheresis therapy is based on physical adsorption. Benefiting from its low side effects and pain attenuation in patients, it has received increasing interest in recent years [7,8]. The key to LDL-apheresis is the preparation of appropriate oil/water separating materials with desirable properties for LDL adsorption. During the past decades, a lot of oil/water separating materials have been developed to adsorb oils, organic compounds, and superfluous lipids from complex oil−water mixtures, either immiscible blends or emulsions [9–11]. Among them, synthetic porous materials, such as aerogels (e.g. graphene sponge and carbon nanotube sponge), exhibit advantageous properties including high porosity, large surface area, stable durability, and most prominently, high adsorption efficiency for lipid, oil, and organic solvents [12–15]. Nevertheless, synthetic material suffers from the harmful precursors, complicated multi-step preparation procedures, and relatively high-cost raw materials and devices involved in the fabrication process, all of which have

* Corresponding author. Precision Medicine Center Laboratory, The First Affiliated Hospital of Wenzhou Medical University, Wenzhou, 325035, China.
** Corresponding author. Precision Medicine Center Laboratory, The First Affiliated Hospital of Wenzhou Medical University, Wenzhou, 325035, China.
*** Corresponding author. Precision Medicine Center Laboratory, The First Affiliated Hospital of Wenzhou Medical University, Wenzhou, 325035, China.
E-mail addresses: luoranshang@fudan.edu.cn (L. Shang), xfxj2000@126.com (J. Xiao), yjzhao@seu.edu.cn (Y. Zhao).

https://doi.org/10.1016/j.bioactmat.2020.11.015
Received 19 September 2020; Received in revised form 5 November 2020; Accepted 9 November 2020
2452-199X/© 2020 The Authors. Production and hosting by Elsevier B.V. on behalf of KeAi Communications Co., Ltd. This is an open access article under the CC BY-NC-ND license (http://creativecommons.org/licenses/by-nc-nd/4.0/).

dramatically hindered its large-scale production and practical applications. To overcome these limitations, many natural adsorbents such as expanded perlite, zeolites, and porous biomass, including wool fiber, activated carbon, and sawdust are constantly applied to treating oil—water blends due to their high porosity, simple fabrication, and abundant source [16–21]. However, these materials still face the dilemma of low oil-water selectivity, insufficient adsorption capacity and poor recyclability, which severely suppress their utilization efficiency. In addition, most of these oil adsorbents are used in bulk, and their motion behaviors are largely limited, thus hampering the adsorption process [22–24]. These drawbacks, together with the unsatisfactory biocompatibility, make the current adsorbent materials hardly eligible in biomedical application scenarios. Therefore, it is strongly desired to design facile, accessible, and low-cost porous adsorbent materials for efficient separation of blood lipids.

In this paper, we develop an ingenious porous adsorbent derived from natural biomass for separating oils, organic compounds, and LDL in blood. Biomass-derived functional materials are cheap, easily accessible, sustainable, and environmentally friendly. The natural pollen grains, characterized by their highly porous structure with numerous voids and high surface areas, play a role in protecting genetic information of plants from harsh environmental conditions [25–27]. Therefore, they are considered as favourable and extremely robust biomass candidates for preparing adsorption materials. Besides, as a typical example of exquisite naturally evolved material, pollen grains possess a large inner cavity, which makes them terrific storage vehicles for the encapsulation of various substances. Furthermore, they are easy to obtain due to the endless supply and can be collected with great ease, thereby greatly reducing the production costs. Profiting by the above intrinsic superiorities, pollens-derived materials have been rifely applied in biomedical field, such as drug delivery, bioassay, and cell recognition [28–33]. Despite that tremendous progress have been made, their potential value in LDL adsorption and retention remains unexplored.

We herein propose a magnetically actuated lacunaris pollen grains with a hollow structure and abundant macropores for adsorbing oils, organic solvents, and LDL in blood, as schemed in Fig. 1. Ordinary pollen grains possess a relatively intact surface with a few pores, and lack the ability of controllable motion, which limit their adsorption performances. Therefore, we modified the natural pollen grains to meet the requirements for oil-water separation and lipid adsorption. Intriguingly, after a simple calcination pretreatment process, the pollen grains exhibited distinct polyporous features on the surface and a central cavity inside. It is worth mentioning that the resultant calcined pollen grains (CPGs) were amphiphilic and can be directly used for absorbing excess lipids in the blood. The adsorbents could be readily parted under magnetic field force for further multiple reuse after they were decorated with magnetic nanoparticles. The LDL level of plasma reduced by 34.9% after dynamic hemoperfusion after 2 h. Besides, through further modification, the CPGs were rendered hydrophobic and were employed as adsorbents for a variety of oil pollutants. The hydrophobic pollen grains (HPGs) were found that they could float on water for long, thus feasible for dealing with the oil slick problems. The adsorption tests revealed that the CPGs and HPGs possessed excellent adsorption capacity, with relatively high selectivity, rapid adsorption, and stable reusability. These merits could be attributed to the pivotal impact of their large pore volumes and outstanding surface areas. Besides, the pollen shells showed a uniform network structure, which served as an excellent oily-liquid transmission channel. These features make the pollens derived magnetic porous particles ideal candidate for removing oil pollutants and blood lipids in practical applications.

2. Experimental section

2.1. Materials

N-hexadecane (98%), acetone, dichloromethane, diiodomethane, Octadecyltrichlorosilane (OTS), and Sudan III were gained from Aladdin Industrial Corporation. Peanut oil and Golden Arowana® blend oil (cooking oil) were purchased from a supermarket in Southeast University. Diesel oil was obtained from Sinopec. The sunflower (*Helianthus annuus*) pollen grains were collected from natural sunflower. The ferromagnetic magnetic nanoparticles were purchased from Nanjing Nanoeast Biotech Co. LTD. Deionized water was purified in a Milli-Q system (Millipore, Bedford, USA) and was used for all experiments. Plasma sample was provided by healthy volunteers and hyperlipemia patients.

2.2. Preparation of the CPGs and the HPGs

The raw pollens were calcined at 800 °C for 12 h to obtain CPGs with porous and hollow structure. Then, 200 mg CPGs were added to 10 mL Fe_3O_4 magnetic nanoparticles dispersion of 100 mg/mL, with shaking

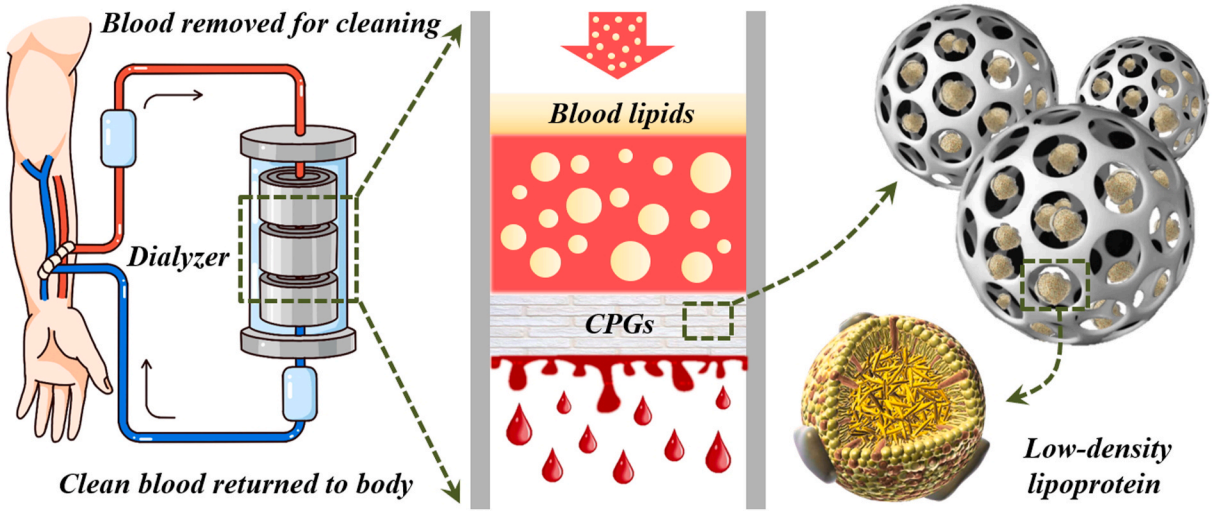

Fig. 1. Schemes of the process of a simulative LDL-apheresis apparatus with CPGs used as the adsorbents. Based on the current clinically applied hemoperfusion technique, hyperlipidemia plasma is drawn from the human body and injected into the dialyzer, which is filled with the adsorbent CPGs. Due to the high porosity and hollow structure of these particles, as well as hydrophobicity, blood lipids can be absorbed into the voids. Generally, after manifold cycles, the purified and filtered low-lipemia plasma can be returned to the body.

for 1 h. A permanent magnet was used to test the magnetic adsorption effect. Subsequently, the magnetic CPGs were collected and dried. The magnetic CPGs were then added to a solution containing 1 vol% OTS in acetone with continuous shaking for 3 h to obtain the HPGs.

2.3. Absorption experiments for oils and organic solvents

Six types of oil/organic solvent-water mixture was prepared. The oils and organic solvents included peanut oil, golden arowana blend oil, diesel oil, hexadecane, acetone, and dichloromethane. 500 mg HPGs were cast onto the oil surface floating on water and allowed for adsorption for 10 min. Then, the adsorbents were taken out and weighed. The adsorption capacity of the HPGs for different pollutants were calculated according to Formula (1). The saturated HPGs were soaked in ethanol, followed by shaking for 1 h. Afterwards, a magnet was used to collect the HPGs and the remaining waste liquid was discarded. The above operations were repeated 3 times to ensure that the HPGs were completely cleaned without the oil residue. Finally, the purified HPGs were dried and utilized for recycling.

2.4. Absorption experiments for LDL from hyperlipemia plasma

Static LDL adsorption test was performed *in vitro* to determine the adsorption and clearance capacity of CPGs. The human plasma sample from hyperlipemia patients was thawed initially in a 37 °C water bath. Then, CPGs (about 1 g in wet weight) were immersed in a 2 mL plasma containing LDL at a much higher level than the clinical normal value. Then they were incubated at 37 °C for 3 h and the supernatants were collected. LDL, TC, TG, and HDL levels of collected supernatants were measured by the full-automatic biochemical analyzer. Five replicates were averaged. Dynamic LDL adsorption test was performed in a hemoperfusion chip and a simulative hemoperfusion column. The chip was composed of Polydimethylsiloxane (PDMS) material fabricated by standard soft lithography. The internal cell of the chip was filled with CPGs. The hyperlipemia plasma was pumped into the catheter linked to the chip, and then flowed through the CPGs. As for the simulative hemoperfusion column, a 5-mL syringe was filled with 2 g dried CPGs. The hyperlipidemia plasma sample flowed through the adsorbent layer under gravity. Then five repeated adsorption procedures were conducted and each lasted about 10 min. Normal saline was applied to flush the column after a plasma purification procedure. Finally, 2 mL of the treated plasma was sucked out for further measurement of lipid profile via the biochemical analyzer mentioned above.

2.5. Characterization

The microstructures of the raw pollens and the treated particles were characterized by the scanning electron microscope (SEM, Hitachi S3000 N) with gold sputter coating, and the atomic concentration of the products was identified using energy dispersive spectrum (EDS) supporting SEM. Blood-related indicators were measured by Cobas 8000 full-automatic biochemical analyzer in Department of Clinical Laboratory of the Affiliated Drum Tower Hospital of Nanjing University Medical School. The pore diameters were measured via the mercury injection apparatus (PoreMaster33GT, Quantachrome). The water contact angle (WCA) and oil contact angle (OCA) were measured applying deionized water drop and diiodomethane droplet at room temperature, with a contact angle meter (Hitachi, CA-A).

3. Results and discussion

In a typical experiment, the CPGs were prepared from sunflower *(Helianthus annuus)* pollen grains after removing the impurities and calcination at 800 °C for 12 h. The raw sunflower pollen grains are microparticles with uniform size ranging from 30 to 40 μm and well-organized morphology consisting of nanoscale-spiny features and a small quantity of pores, as shown in Fig. S1. After high-temperature calcination, most of organic matter of the pollen grains were removed. Compared with raw pollen grains, the CPGs exhibited highly porous morphologies at the surface and a central hollow cavity inside, as shown in the SEM images in Fig. 2a and b. The shell of the CPGs displayed a uniform network structure, and this could serve as an excellent oily-liquid transmission channel, as well as providing high specific surface area. The shrinkage and pores-formation of the pollen were resulted from the removal of the organic matter in their cytoplasmic core, cellulosic intine layer, and the outermost exine layer containing the sporopollenin biopolymer after calcining. The *in situ* element analysis results (Fig. 2d) indicated that the calcined pollens are mainly composed of inorganic substances, including calcium, phosphorus, and potassium. Mercury Intrusion Capillary Pressure (MICP) was measured to determine the pore size distribution of the CPGs, as shown in Fig. 2e. The specific pores area was 1.68 m^2/g. It can be concluded from the curve that the CPGs had a narrow pore-size distribution centralised in the 0.5–3 μm range with a peak at 1.18 μm, demonstrating the presence of mesoporous in the CPGs. The high specific surface area and big holes are conducive to the adsorption course, providing more contact sites and faster adsorption rate. The porous structure and large surface area of these calcined particles allowed for the adsorption of Fe_3O_4 nanoparticles at the surface and interior of the CPGs (Fig. 2c), which endowed the CPGs with magnetic response property. As shown in the insets of Fig. 2f, the magnetic CPGs could be controlled to move toward one side of a vial by using a permanent magnet. Meanwhile, the results of EDS analysis also proved the increase of iron content in the sample (Fig. 2f).

To impart CPGs with more applicative wettability characteristics, reinforced hydrophobic pollen grains (HPGs) were prepared through surface activation and Octadecyltrichlorosilane (OTS) modification. Contact angle were measured on both CPGs and HPGs applying deionized water and diiodomethane using sessile drop method, as shown in Fig. 3. Thin layers of the CPGs were obtained through attaching their dry powder to a glass slide with a double-faced adhesive tape. As shown in Fig. 3a and b, the droplet quickly subsided into CPGs upon contacting the powder layer, thus it had no time to measure the static contact angle because of the rapid penetration. The value of water contact angle (WCA) of the magnetic CPGs was about 10.76° (Fig. 3c and d), indicating a salient hydrophilic performance. Surprisingly, the oil contact angle (OCA) of the magnetic CPGs was 19.75° (Fig. 3e and f), which manifested the amphiphilic feature of the CPGs. The unmodified calcined porous pollen grains appeared white due to the removal of colored organic matter, while they turned into light brown after absorbing Fe_3O_4 nanoparticles.

To further confirm this, we studied the wetting preferences of the CPGs at an oil-water interface in a vial. A mixture containing an upper layer of *n*-hexadecane and a lower layer of deionized water was prepared first, and CPGs were slowly released to the uppermost layer of each liquid surface. The CPGs did not maintain floating at the oil phase, but continued to sink across the oil-water interface, and finally settled to the bottom of the water layer (Fig. 3i and j). We then prepared another mixture containing an upper layer of water and a lower layer of chloroform, and repeated the above operation. It was found that the CPGs deposited to the water-oil interface and remained pinned at the interface instead of submerging (Fig. 3k, l). It could thus be concluded that the CPGs possess water and oil amphiphilic properties, but they are comparatively more hydrophilic. This was consistent with the contact angle measurements. On the contrary, the WCA of the HPGs was measured to be 147.07°, suggesting their absolute hydrophobic property (Fig. 3g and h). Fig. S2a presented that the water drop could stay on HPGs without significant change in over 5 min. Compared with the CPGs, the surface of HPGs possessed hydrophobic alkane chains after OTS modification. To take further advantage of their hydrophobicity, we used the HPGs to coat 5 μL water droplet, and formed the "liquid marbles" (i.e. non-stick liquid drops wrapped by a hydrophobic powder).

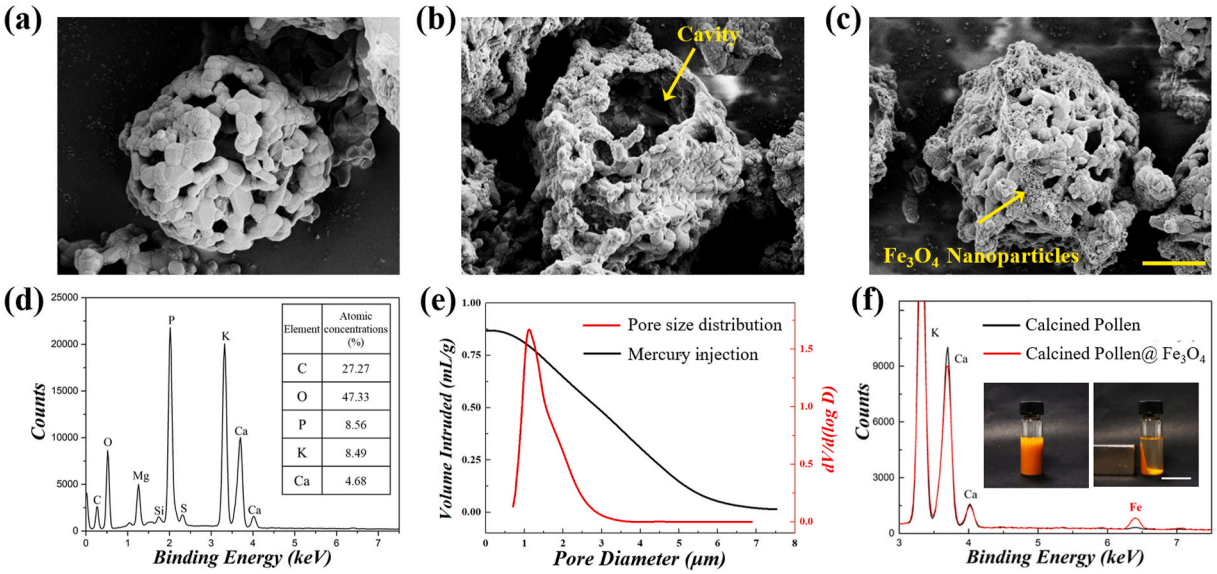

Fig. 2. (a–c) SEM images of (a) the CPGs exhibiting their highly porous morphologies at the surface, (b) a central hollow cavity inside, and (c) the CPGs adsorbed with Fe_3O_4 nanoparticles. (d) EDS of the CPGs and their atomic concentrations. (e) Mercury injection curve and the corresponding pore size distribution curve of the CPGs, showing a well-defined characteristic pore size of 0.5–3 μm. (f) The EDS curves showing variations on Fe counts in the CPGs after adsorbing Fe_3O_4 nanoparticles. The insets showed strong magnetic responsiveness of the CPGs with Fe_3O_4 nanoparticles deposited. The pollen grains were dispersed in the solution and then collected to one side of a vial by a magnet. Scale bars are 1.5 μm in (a–c) and 4 cm in (f).

The as-prepared liquid marbles were steady and kept intact even after being transferred onto a hydrophilic glass substrate or water surface, thus facilitating their applications in more complicated oil-water separation, as shown in Figs. S2b and 2c.

To verify the actual effects of the magnetic porous pollen grains for water purification, HPGs were utilized for adsorbing the surface oil on water. As shown in Fig. 4a, a glass culture dish containing red-dyed *n*-Hexadecane floating on water was prepared. The magnetic-incorporated HCPs were then added to the mixture. Fig. 4b–e showed the process of n-Hexadecane gathering around the particles and gradually being absorbed, and finally no colored organic solvent could be observed. Besides, the HPGs floated on the liquid surface for a long time and the whole adsorption process took approximately 30 s. At the last procedure, due to the existence of Fe_3O_4 nanoparticles, HPGs could be controllably moved to one side of the container with an external magnet (Fig. 4f). Thus, in the actual scene, the HPGs could be first cast onto the water surface at a random dispersion and then moved to the targets. This ability not only increases the adsorption efficiency, but also facilitates the collection and recovery of the adsorbents and their captured targets. Hence, the magnetic porous pollen grains are promising to remove toxic oily liquids in water treatment.

To explore the adsorption capacity of the HPGs for various oily liquids, several oil and organic solvent adsorption experiments were conducted. The sorption capacity of the adsorbent was expressed as the amount of pollutant adsorbed divided by the amount of the adsorbent:

$$D_{eq} = \frac{(w_e - w_0)}{w_0} \quad (1)$$

where D_{eq} is the sorption capacity of the adsorbent, w_e is the mass of the adsorbent at equilibrium, and w_0 is the primary mass of the adsorbent. Fig. 4g presents the maximum oil adsorption capacity of the HPGs for different organic solvents and oils, respectively. The adsorption capacity for organic solvents were much higher than that of the oils selected. The adsorption capacity of the HPGs for oils and organic solvents ranged from 17.8 to 58.4 g/g and 13.9–22.3 g/g, respectively. The differences could be ascribed to the density, surface energy, and viscosity diversity of the oils and organic solvents. The adsorption ability of the HPGs was significantly improved compared with the hydrophobized raw pollen grains without calcination. The oil adsorption capacity variation could be explained that the adsorption mechanism can be ascribed to the spacial storage of oil across the interconnected pores at the surface toward the interior cavity of the pollens, and this process relies on the capillary force. The capillary flow was strengthened by the oleophilic surface when the oils spread into the pores. Thus, the high porosity of the HPGs could provide more adsorption space compared with the raw pollen grains. In general, HPGs can take up these oils and solvents at 13–59 times its own weight and their adsorption capacities are much higher than those of established absorbents derived from natural inorganics and biomass, as listed in Table S1 [34–37]. Compared with synthetic absorption materials such as spongy graphene and carbon fiber aerogel, HPGs have lower capacity due to the relatively lower porosity and specific surface area. However, the naturally derived HPGs are superior over other synthetic absorbents because of the low cost, abundant sources, and simple synthesis procedure. The conclusion drawn from the adsorption performances above is that the HPGs have great potential to be an outstanding adsorbent and can be utilized for the treatment of oily wastewater, removal of mechanical resid, cleaning of kitchen grease, etc.

The recyclability and the removal efficiency of the HPGs absorbent play important roles in pollution control and environment protection. For this purpose, the repeatability of the HPGs for the adsorption and desorption of oil and organic solvents was tested for eight cycles. As illustrated in Fig. 5a–d, the adsorbed substance could be easily removed from HPGs by washing in ethanol. Following that, the recovered pristine HPGs were collected and subsequently dried under vacuum. Then the prepared particles could be repeatedly used. Fig. 5e presented that the HPGs' absorption capacity for hexadecane could recover almost 100% after eight absorption−harvesting cycles. During the cycles, HPGs maintained the stability in size and structure, and there was no oil residue inside. The outstanding stability and durable service life of HPGs not only avoided secondary pollution but also saved the adsorbent materials for repeated use.

LDL plays the role of primary carrier for plasma cholesterol in mankind and one of the pivotal factors of the development of atherosclerosis. LDL-apheresis therapy is confirmed efficient for treating familial hypercholesterolemia patients and the group of people for whom

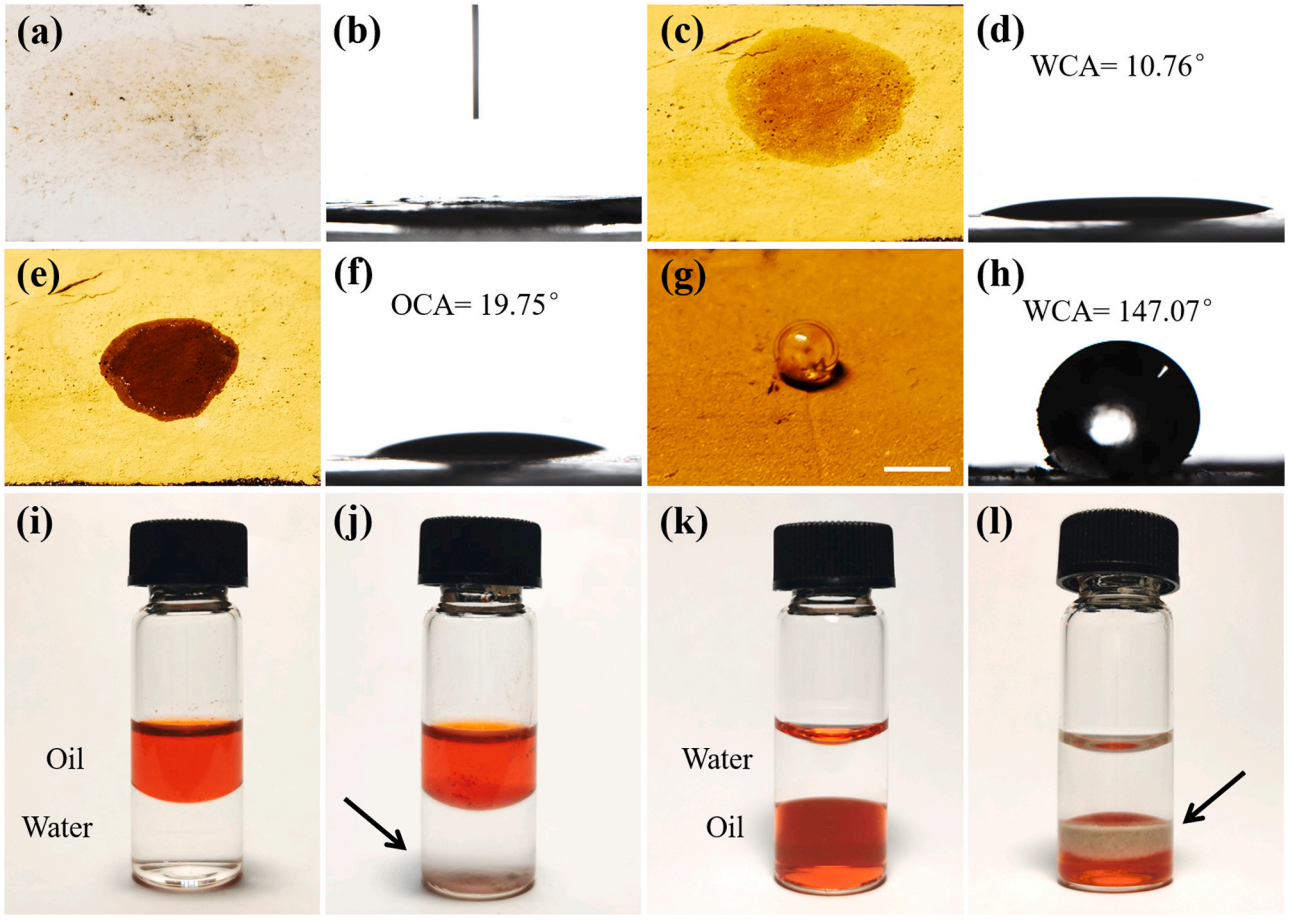

Fig. 3. Water and oil contact angle measurements of the CPGs and HPGs. (a) The CPGs have a hydrophilic surface and can be wetted by water droplets. (b) The image showing the water droplet immediately penetrated the CPGs layer. (c–f) Photographs of the magnetic CPGs absorbed with Fe_3O_4 nanoparticles and their state of being wetted by (c) deionized water, and (e) diiodomethane. The corresponding (d) WCA value was 10.76°, and the (f) OCA value was 19.75°. (g, h) After treatment with OTS, the resultant HPGs become hydrophobic with an WCA value of 147.07°. (i–l) Pictures showing the CPGs' amphipathic performance. (i, j) The upper layer was red-dyed *n*-hexadecane and the lower layer was deionized water. (k, l) The upper layer was deionized water and the lower layer was a red-dyed chloroform. The arrows indicated the location of the CPGs. The scale bars are 1 cm in (a, c, e, and g).

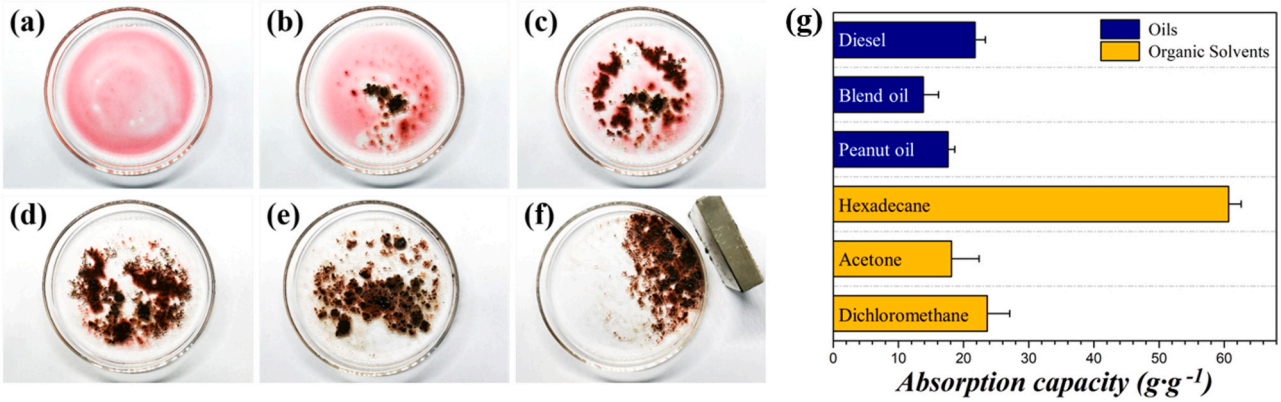

Fig. 4. (a–f) Photographs illustrating the adsorption stages of *n*-Hexadecane (red-dyed by Sudan III) floating on the water surface by using HPGs. The adsorbed *n*-Hexadecane-HPGs complexes could be controllably dragged to one side with an external magnet. (g) Absorption capacities of HPGs for typical oils and organic solvents, including diesel, blend oil, peanut oil, and hexadecane, acetone, dichloromethane, respectively.

the diet or medication cannot work. It is a technique in forms of extra-corporeal lipoprotein elimination, where the key lies in the appropriate adsorbents. In this work, the CPGs were chosen as novel LDL adsorbents, due to their superior amphipathic feature. A static and dynamic LDL adsorption test were carried out *in vitro* to determine the adsorption and clearance capacity of the CPGs for the hyperlipidemia plasma. Fig. 6a illustrated the time-dependent adsorption profiles of CPGs regarding the removal of LDL, high-density lipoprotein (HDL), triglyceride (TG), and cholesterol (TC). Approximately 29.7% of LDL in plasma was eliminated by CPGs in the initial 1 h. As for HDL, the adsorption efficiency of CPGs

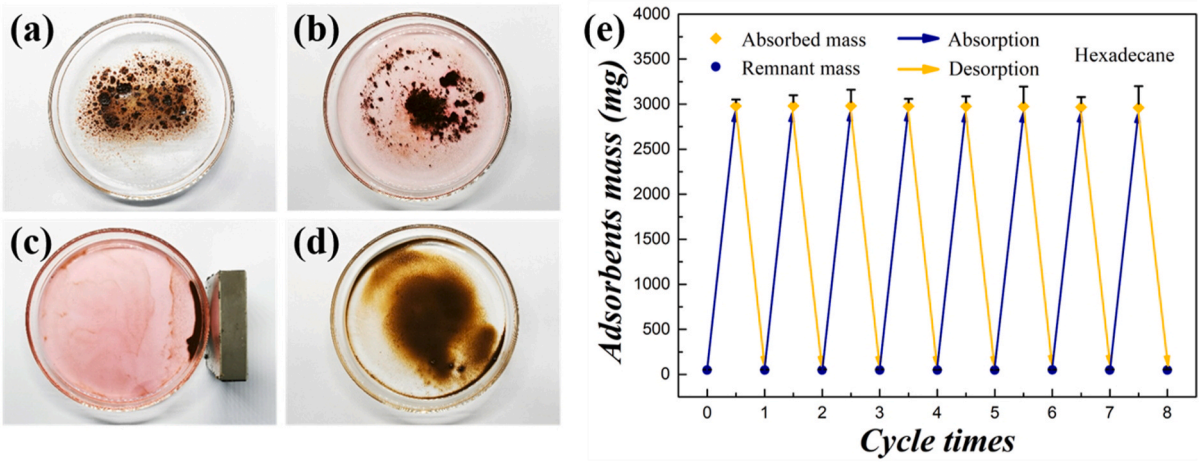

Fig. 5. (a–d) Photographs showing the recycle procedures of HPGs for the adsorption and desorption of hexadecane. (a) The HPGs absorbed saturated n-hexadecane were immersed in ethanol. (b) Gradually, the red-dyed organic solvent was dissolved out. (c) Afterwards, a magnet was used to collect the HPGs and the remaining waste liquid was discarded. (d) The completely cleaned HPGs were dried for recycling use. (e) The repeatability test of the HPGs for the hexadecane adsorption for 8 cycles.

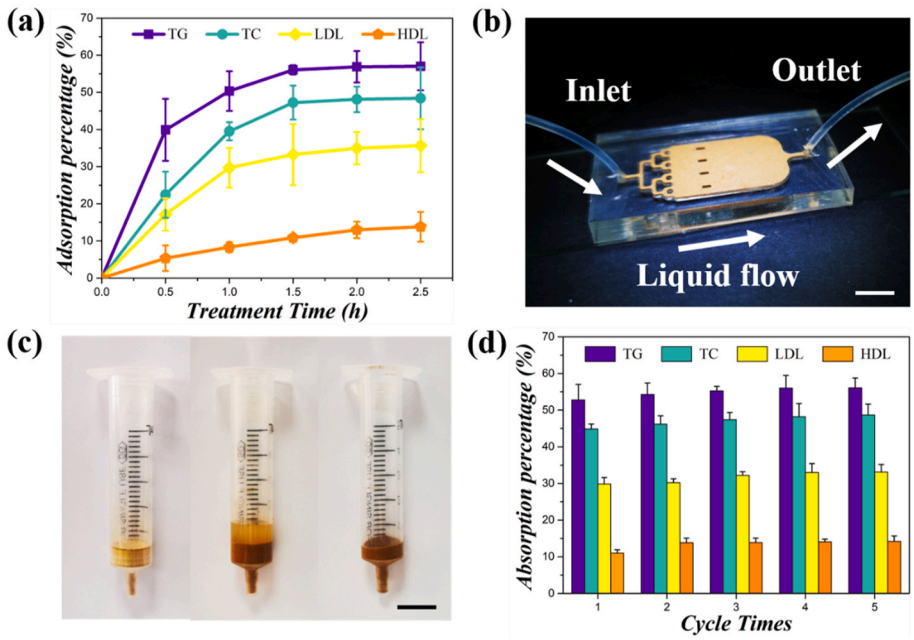

Fig. 6. CPGs for the LDL adsorption in plasma. (a) The time-dependent static adsorption curve illustrating the adsorption capacity of CPGs for TG, TC, LDL, and HDL in hyperlipidemia plasma. (b) The dynamic adsorption test conducted in a hemoperfusion chip. The arrows indicated the inlet, outlet of the chip, and the direction of liquid flow. (c) The simulative hemoperfusion column for LDL adsorption. (d) The dynamic adsorption graph for LDL, HDL, TG, and TC removal by CPGs in five cycles. Scale bars are 1 cm in (b), and 2 cm in (c).

was around 8.3%, suggesting that the CPGs could effectively remove LDL without significant adsorption of HDL, and meet the clinical requirement for lipid reduction. The adsorption reached a plateau after 2.5 h' adsorption. The results revealed that the CPGs had definite adsorption selectivity for LDL removal, with an adsorption capacity of around 8.65 mg/g. Interestingly, the adsorbed amount of TC and TG was larger than that of LDL, which might because of the higher original levels of the two in the plasma sample. We investigated the adsorption selectivity of the CPGs using a simplified column model and a hemoperfusion chip, as shown in Fig. 6b and c. The chip was made of PDMS material fabricated by standard soft lithography. The adsorbents CPGs was loaded in the internal cell of the chip. The hyperlipemia plasma was injected into the catheter linked to the chip, and then flowed through the CPGs. As for the simulative hemoperfusion column, a 5-mL syringe was filled with 2 g dried CPGs to form an adsorption column. Then five repeated adsorption procedures were conducted and each lasted about 10 min. The hyperlipidemia plasma sample flowed through the adsorbent layer filled with CPGs under gravity. As shown in Fig. 6d, the adsorption percentage of LDL in plasma increased from 29.8% to 33.6% while that of HDL displayed a slight fluctuation. The adsorption capacity of the CPGs in the dynamic adsorption test was about 12.87 mg/g after a 50-min simulative hemoperfusion treatment. We thus anticipate that, with a longer treatment time (for example, as long as 3 h in real clinical practice), greater adsorption clearance and capacity would be achieved. The extraordinary adsorption performance could be attributed to the increased amount of adsorption sites brought by the high porosity and good amphipathy of these porous particles.

To confirm the hemocompatibility of the CPGs, we evaluated the hemolysis ratio (HR), anticoagulation, and platelet adhesion. The CPGs were incubated with blood obtained from healthy volunteers, and the value of HR, prothrombin time (PT), activated partial thromboplastin time (APTT), and thrombin time (TT) of the sample were measured. Table 1 demonstrated the value was within the clinical limits, indicating a good hemocompatibility of the CPGs. In addition, the platelet adhesion

Table 1
The hemolysis ratio (HR), prothrombin time (PT), activated partial thromboplastin time (APTT), and thrombin time (TT) of CPGs.

Materials	HR (%)	PT (s)	APTT (s)	TT (s)
CPGs	1.32 ± 0.39	11.4 ± 0.5	32.7 ± 3.9	13.3 ± 1.2
CPGs@Fe_3O_4	1.02 ± 0.21	10.9 ± 2.3	30.3 ± 3.2	12.5 ± 2.1

assay was conducted. Fig. S3 shows the optical microscopic images of platelet adhesion when 100 mg of the CPGs were added to 1.0 mL platelet-rich plasma, and the platelets were not significantly activated. All these tests suggested the potential clinical application for LDL removal from plasma.

4. Conclusion

In summary, we have successfully developed a pollen grains-derived, magnetic porous material for oil pollutants and LDL adsorption. The pollen grains after calcination treatment exhibited large pore volumes and abundant surface areas, and Fe_3O_4 nanoparticles could be incorporated via physical adsorption to generate magnetic responsiveness feature. Then the magnetic calcinated pollen grains were treated hydrophobic. The resultant particles demonstrated excellent oils/organic solvents adsorption performance, with a highly-efficient and selective adsorption capacity achieved, compared with those of established absorbers derived from representative natural inorganics and biomass. Besides, the adsorption capacity of the particles remained unchanged after more than 8 adsorption cycles. In addition, the simple calcined pollen grains exhibited biocompatible properties in blood, and an ideal adsorption capacity of LDL. Given its excellent reusability and durability, the novel pollen-derived, magnetic porous material is promising for oil-water separation, safe blood lipid adsorption in plasma, and the associated biomedical applications.

CRediT authorship contribution statement

Yuetong Wang: conducted experiments and data analysis, Writing - original draft. **Lingyu Sun:** Writing - original draft. **Jiahui Guo:** Writing - original draft. **Keqing Shi:** Writing - original draft. **Luoran Shang:** Writing - original draft. **Jian Xiao:** Writing - original draft. **Yuanjin Zhao:** conceived the idea and designed the experiment, Writing - original draft.

Declaration of competing interest

The authors declare that they have no known competing financial interests or personal relationships that could have appeared to influence the work reported in this paper.

Acknowledgment

This work was supported by the National Key Research and Development Program of China (2020YFA0908200), the National Natural Science Foundation of China (52073060, 22002018, 81800567 and 61927805), the Natural Science Foundation of Jiangsu (BE2018707), and the Launching Funds from Fudan University (JIH1340032 and JIH1340038) and the affiliated Zhongshan-Xuhui Hospital (KJK04202000021).

Appendix A. Supplementary data

Supplementary data to this article can be found online at https://doi.org/10.1016/j.bioactmat.2020.11.015.

References

[1] P.A. Kiberstis, Fatty liver- too much of a bad thing? Science 14 (364) (2019) 1044–1045.
[2] D. Vojinovic, D. Radjabzadeh, A. Kurilshikov, N. Amin, C. Wijmenga, L. Franke, M. A. Ikram, A.G. Uitterlinden, A. Zhernakova, J. Fu, R. Kraaij, C.M. Duijn, Relationship between gut microbiota and circulating metabolites in population-based cohorts, Nat. Commun. 10 (2019) 5813.
[3] J.H. Thierer, S.C. Ekker, S.A. Farber, The LipoGlo reporter system for sensitive and specific monitoring of atherogenic lipoproteins, Nat. Commun. 10 (2019) 1–14.
[4] J.M. Johnston, A. Angyal, R.C. Bauer, S. Hamby, S.K. Suvarna, K. Baidžajevas, Z. Hegedus, T.N. Dear, M. Turner, , The Cardiogenics Consortium, H.L. Wilson, A. H. Goodall, D.J. Rader, C.C. Shoulders, S.E. Francis, E.K. Toth, Myeloid Tribbles 1 induces early atherosclerosis via enhanced foam cell expansion, Sci. Adv. 5 (10) (2019), eaax9183.
[5] Y. Li, M. Han, Y. Wang, Q. Liu, W. Zhao, B. Su, C. Zhao, A mussel-inspired approach towards heparin-immobilized cellulose gel beads for selective removal of low density lipoprotein from whole blood, Carbohydr. Polym. 202 (2018) 116–124.
[6] L. Merolle, C. Marraccini, A. Latorrata, E. Quartieri, D. Farioli, L. Scarano, T. Fasano, S. Bergamini, E. Bellei, E. Monari, A. Tomasi, E. Di Bartolomeo, R. Baricchi, T. Pertinhez, Heparin-induced lipoprotein precipitation apheresis in dyslipidemic patients: a multiparametric assessment, J. Clin. Apher. 35 (3) (2020) 146–153.
[7] X. Ho, T. Zhang, A. Cao, A heparin modified polypropylene non-woven fabric membrane adsorbent for selective removal of low density lipoprotein from plasma, Polym. Adv. Technol. 24 (2013) 660–667.
[8] Y. Liu, W. Qiu, H. Yang, Y. Qian, X. Huang, Z. Xu, Polydopamine-assisted deposition of heparin for selective adsorption of low-density lipoprotein, RSC Adv. 5 (2015) 12922.
[9] W. Ma, Y. Li, M. Zhang, S. Gao, J. Cui, C. Huang, G. Fu, Biomimetic durable multifunctional self-cleaning nanofibrous membrane with outstanding oil/water separation, photodegradation of organic contaminants, and antibacterial performances, ACS Appl. Mater. Interfaces 12 (2020) 34999–35010.
[10] C. Li, G. Shi, Functional gels based on chemically modified graphenes, Adv. Mater. 26 (2014) 3992.
[11] L. Huang, L. Zhang, J. Song, X. Wang, H. Liu, Superhydrophobic nickel-electroplated carbon fibers for versatile oil/water separation with excellent reusability and high environmental stability, ACS Appl. Mater. Interfaces 12 (2020) 24390–24402.
[12] C. Tan, X. Cao, X. Wu, Q. He, J. Yang, X. Zhang, J. Chen, W. Zhao, S. Han, G. Nam, M. Sindoro, H. Zhang, Recent advances in ultrathin two-dimensional nanomaterials, Chem. Rev. 117 (2017) 6225–6331.
[13] Y. Zhao, C. Yu, H. Lan, M. Cao, L. Jiang, Improved interfacial floatability of superhydrophobic/superhydrophilic janus sheet inspired by lotus leaf, Adv. Funct. Mater. 27 (2017) 1701466.
[14] J. Ge, H. Zhao, H. Zhu, J. Huang, L. Shi, S. Yu, Advanced sorbents for oil-spill cleanup: recent advances and future perspectives, Adv. Mater. 28 (2016) 10459.
[15] J. Fan, J. Luo, Z. Luo, Y. Song, Z. Wang, J. Meng, B. Wang, S. Zhang, Z. Zheng, X. Chen, S. Wang, Bioinspired microfluidic device by integrating a porous membrane and heterostructured nanoporous particles for biomolecule cleaning, ACS Nano 13 (7) (2019) 8374–8381.
[16] D. Bastani, A. Safekordi, A. Alihosseini, V. Taghikhani, Study of oil sorption by expanded perlite at 298.15 K, Sep. Purif. Technol 52 (2006) 295–300.
[17] T. Sakthivel, D. Reid, I. Goldstein, L. Hench, S. Seal, Hydrophobic high surface area zeolites serived from fly ash for oil spill remediation, Environ. Sci. Technol. 47 (2013) 5843–5850.
[18] M. Radetic, V. Ilic, D. Radojevic, R. Miladinovic, D. Jocic, P. Jovancic, Efficiency of recycled wool-based nonwoven material for the removal of oils from water, Chemosphere 70 (2008) 525–530.
[19] M. Buzaeva, E. Kalyukova, E. Klimov, Treatment of oil spill by sorption technique using fatty acid grafted sawdust, Russ. J. Appl. Chem. 83 (2010) 1883–1885.
[20] L. Sun, J. Wang, Y. Yu, F. Bian, M. Zou, Y. Zhao, Graphene oxide hydrogel particles from microfluidics for oil decontamination, J. Colloid Interface Sci. 528 (2018) 372–378.
[21] Y. Li, Y.A. Samad, K. Polychronopoulou, S.M. Alhassan, K. Liao, Carbon aerogel from winter melon for highly efficient and recyclable oils and organic solvents absorption, ACS Sustain. Chem. Eng. 2 (6) (2014) 1492–1497.
[22] Y. Wang, Q. Li, L. Bo, X. Wang, T. Zhang, S. Li, P. Ren, G. Wei, Synthesis and oil absorption of biomorphic MgAl Layered Double Oxide/acrylic ester resin by suspension polymerization, Chem. Eng. J. 15 (284) (2016) 989–994.
[23] S.S. Elanchezhiyan, N. Sivasurian, S. Meenakshi, Recovery of oil from oil-in-water emulsion using biopolymers by adsorptive method, Int. J. Biol. Macromol. 70 (2014) 399–407.
[24] Q. Yu, Y. Zheng, Y. Wang, L. Shen, H. Wang, Y. Zheng, N. He, Q. Li, Highly selective adsorption of phosphate by pyromellitic acid intercalated ZnAl-LDHs: assembling hydrogen bond acceptor sites, Chem. Eng. J. 260 (2015) 809–817.
[25] Y. Wang, Y. Wang, F. Bian, L. Shang, Y. Shu, Y. Zhao, Quantum dots integrated biomass pollens as functional multicolor barcodes, Chem. Eng. J. 1 (395) (2020) 125106.
[26] R.C. Mundargi, M.G. Potroz, J.H. Park, J. Seo, E.L. Tan, J.H. Lee, N.J. Cho, Eco-friendly streamlined process for sporopollenin exine capsule extraction, Sci. Rep. 6 (2016) 19960.
[27] R.C. Mundargi, M.G. Potroz, S. Park, H. Shirahama, J.H. Lee, J. Seo, N.J. Cho, Natural sunflower pollen as a drug delivery vehicle, Small 12 (2016) 1167–1173.

[28] Y. Wang, L. Shang, G. Chen, C. Shao, Y. Liu, P. Lu, F. Rong, Y. Zhao, Pollen-inspired microparticles with strong adhesion for drug delivery, Appl. Mater. Today 13 (2018) 303–309.
[29] I. Sargin, L. Akyuz, M. Kaya, G. Tan, T. Ceter, K. Yildirim, S. Ertosun, G.H. Aydin, M. Topal, Controlled release and anti-proliferative effect of imatinib mesylate loaded sporopollenin microcapsules extracted from pollens of Betula pendula, Int. J. Biol. Macromol. 105 (2017) 749.
[30] L. Akyuz, I. Sargin, M. Kaya, T. Ceter, I. Akata, A new pollen-derived microcarrier for pantoprazole delivery, Mater. Sci. Eng. C 71 (2016) 937.
[31] M.J. Uddin, H.S. Gill, Ragweed pollen as an oral vaccine delivery system: mechanistic insights, J. Contr. Release 268 (2017) 416.
[32] H. Wang, M.G. Potroz, J.A. Jackman, B. Khezri, T. Marić, N.J. Cho, M. Pumera, Bioinspired spiky micromotors based on sporopollenin exine capsules, Adv. Funct. Mater. 27 (32) (2017) 1702338.
[33] W. Wang, G. Yang, H. Cui, J. Meng, S. Wang, L. Jiang, Bioinspired pollen-like hierarchical surface for efficient recognition of target cancer cells, Adv. Healthc. Mater. 6 (2017) 1700003.
[34] S. Banerjee, M. Joshi, R. Jayaram, Treatment of oil spill by sorption technique using fatty acid grafted sawdust, Chemosphere 64 (2006) 1026–1031.
[35] X. Gui, J. Wei, K. Wang, A. Cao, H. Zhu, Y. Jia, Q. Shu, D. Wu, Carbon nanotube sponges, Adv. Mater. 22 (2010) 617.
[36] H. Bi, X. Xie, K. Yin, Y. Zhou, S. Wan, L. He, F. Xu, F. Banhart, L. Sun, R. Ruoff, Spongy graphene as a highly efficient and recyclable sorbent for oils and organic solvents, Adv. Funct. Mater. 22 (2012) 4421–4425.
[37] H. Bi, Z. Yin, X. Cao, X. Xie, C. Tan, X. Huang, B. Chen, F. Chen, Q. Yang, X. Bu, X. Lu, L. Sun, H. Zhang, Carbon fiber aerogel made from raw cotton: a novel, efficient and recyclable sorbent for oils and organic solvents, Adv. Mater. 25 (2013) 5916–5921.